

Supplemental Material: Pressure-induced Frustration of Magnetic Coupling in Elemental Europium

Shu-Ting Pi,^{1,*} Sergey Y. Savrasov,¹ and Warren E. Pickett^{1,†}

¹*Department of Physics, University of California Davis, Davis, California 95616 USA*

(Dated: December 26, 2018)

TABLE I. Crystal structures of Eu metal at the pressures indicated. x, y, z are the Wyckoff positions, and there are 1, 2 and 4 atoms per primitive cell, respectively. The structural information is taken from Ref. 16 of the manuscript.

P =	4 GPa	14 GPa	75 GPa
Structure	$Im\bar{3}m$ <i>bcc</i>	$P6_3/mmc$ <i>hcp</i>	$Pnma$ orthorhombic
Lattice constants (\AA)	a=4.1961	a=3.3501 b=3.3501 c=5.2962	a=4.977 b=4.264 c=2.944
x	0	1/3	0.325
y	0	2/3	1/4
z	0	1/4	0.029

I. SUPPORTING INFORMATION

A. Structural Information

Like all Ln metals, Eu displays structural transformations with increasing pressure. The bcc phase extends from 0-12 GPa. The common bcc-to-hcp transition for Ln metals occurs at 12 GPa, with single phase hcp in the 12-18 GPa range. The 18-66 GPa regime is more complex, with mixed-phases reported by Husband *et al.*, Ref. 28 of the manuscript. Above 66 GPa, a single phase $Pnma$ regime is reached, which covers the pressure range of interest here. We will simplify and consider the structures as three stages: bcc, 0-12 GPa; hcp, 12-40 GPa; $Pnma$, > 40 GPa. In Table I the experimental lattice structures at specific pressures are listed.

B. $4f$ Charge and Moment versus Pressure

We provide the integrated $4f$ charge, and the total magnetic moment including conduction electron polarization, within the non-overlapping atomic muffin-tin spheres of fixed radius as a function of pressure, in Fig. 1. Since by AFM symmetry all moments have the same magnitude, we only plot the results on one spin-up site. Figs. 1(a), (b) and (c) present these moments versus volume in the bcc, hcp and $Pnma$ structures, respectively, for three values of U . Volumes between the red dashed lines are the experimentally stable regions. Increasing the Hubbard U makes the occupied f -electron orbitals somewhat more localized as expected, by a small

amount weakly dependent on volume. Pressure, by contrast, somewhat expands the $4f$ orbital and decreases the $4f$ charge in the sphere, but only by about 0.5% between 40 and 92 GPa. Differences also arise due to increasing coupling of $4f$ orbitals to conduction states. We conclude that Eu remains in the $4f^7$ configuration in all cases we have studied.

The changes in magnetic moments shown in Fig. 1 (b), (d), and (f) include the change in $4f$ charge (all majority spin) and the change in conduction electron polarization within the sphere. Thus increasing pressure to the 100 GPa range does not change the magnitude of the moments appreciably.

C. L(S)DA+U Method

It is worthwhile to clarify the L(S)DA+U method and the energetic positions of the orbitals treated with this method, in our case it is the Eu $4f$ levels, which are highly localized (the bands are flat). We can compare our result at zero pressure with Kuneš and Laskowski, now our Ref. 27 in the main text, who obtained the $4f$ level at -3 eV with a related calculation. Both calculations used a full potential, all-electron code with no spin-orbit coupling (due to specifications of the spin-coupling methods). They used the Anisimov *et al.* fully localized limit (FLL) form of +U functional, while we used the Dudarev *et al.* form (referenced in the main article) coded in the LMTO code. The spherical f^7 ion of Eu is a case in which the spherical averaging in the Dudarev method has no effect, so this difference is not the source of the different positions in energy of $4f$ levels.

The difference then must be because Kuneš and Laskowski used LDA (this was not specifically stated in their paper) whereas we used LSDA in the underlying DFT functional. It has been stated in the main text why: there is negligible hybridization between the f orbitals and d orbitals, so coupling through the conduction states is initiated by the intra-atomic $d-f$ exchange splitting quantified from a ferromagnetic alignment calculation to be close to 1 eV, as shown in Fig. 2 and Fig. 3. The associated differences in the exchange potentials, arising from the large f spin moment and the nearly $1\mu_B$ d moment, therefore accounts for the difference in $4f$ level positions.

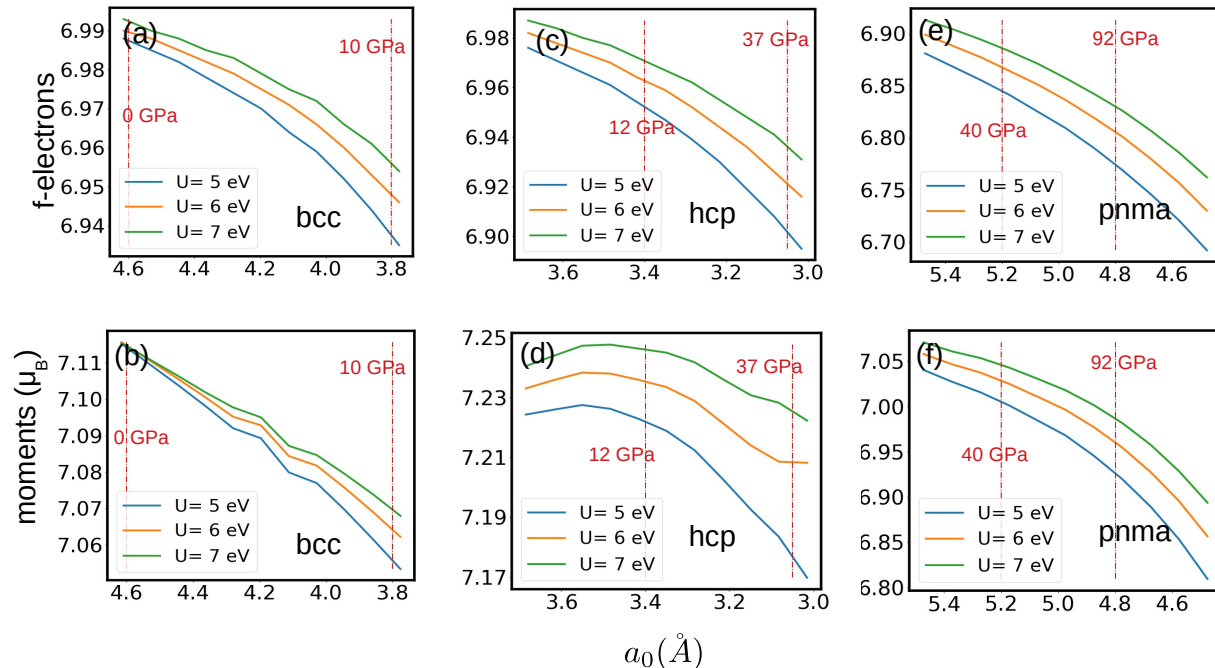


FIG. 1. (Color online) The Eu $4f$ electronic charge, hence also the $4f$ spin moment (top panels), and the total moment within the muffin-tin sphere, versus volume, for the given values of the Hubbard U , in the bottom panels. (a) for the low pressure *bcc* phase, (b) for the intermediate pressure *hcp* phase, and (c) for the high pressure *Pnma* phase. The vertical red lines denote the range of stability of the respective phases. The vertical axis is the a lattice parameter in each structure. All calculations are based on underlying AFM order, the charges and moments are per Eu atom.

D. $4f$ States Position versus Pressure

The position in energy of the $4f$ bands and their localization, and the changes with pressure, are the questions to be discussed here. For orientation, we first provide in Fig. 2 the s , p , d , and f projected densities of states (PDOS) for ferromagnetic spin alignment at zero pressure. The s and p contributions are very minor at the Fermi level and above, leaving the itinerant bands to be almost entirely $5d$ in character. The splitting of the majority and minority d peaks near E_F is almost 1 eV, reflecting intra-atomic exchange coupling between f and d atomic orbitals.

Fig. 4 displays the DFT+ U bands ($U=7$ eV) for each of the structural phases *bcc*, *hcp*, and *Pnma*, at volumes (pressures) near the edges of their range of stability. Figure 4 (a) and (b) show *bcc* bands at 0 and 10 GPa, panels (c) and (d) show *hcp* bands at 12 and 37 GPa, and panels (e) and (f) display *Pnma* phase bands at 40 and 92 GPa. Since the crystal symmetries get progressively lower in this sequence, the bands become successively more complex. To study how the spins are populated, in each case we have projected the band structure on a spin-up site in the AFM ordered cell, with the green regions indicating the extent of the $4f$ spectrum. The $4f$ bands are centered at -6 eV (all energies are referenced

to the Fermi level $E_F=0$) at ambient pressure, but still remain centered at -5 eV at 92 GPa. This represents only a small change in binding energy. The majority $4f$ bands are completely occupied, the minority states are unoccupied; the f^7 configuration seems far from any noticeable change. For the unoccupied states lie at roughly $U+6J$ higher energy, only just becoming visible at the top of the band plots (as red bands).

Note also that little hybridization between $4f$ and $5d$ bands can be seen, as the $4f$ bands lie below (or at the bottom edge of) the itinerant bands. In 92 GPa case some hybridization appears, widening the $4f$ bands somewhat. Reducing the volume increases the conduction electron density, which will provide more screening and reduce the value of U . We have therefore checked the electronic structure for $U = 6, 5$, and 4 eV, but no significant changes on their electronic behaviors were observed. Therefore, based on our calculations, de-occupying a $4f$ orbital seems energetically much too costly to consider, and the magnetic moments remain stable to 92 GPa and probably well beyond. Elemental Gd has a similar $4f^7$ configuration, and DFT+ U calculations indicated no valence transition would occur until well above 500 GPa (see the main text for discussion and references). We conclude that the superconductivity that emerges at 82 GPa is not induced, or one might say enabled, by a

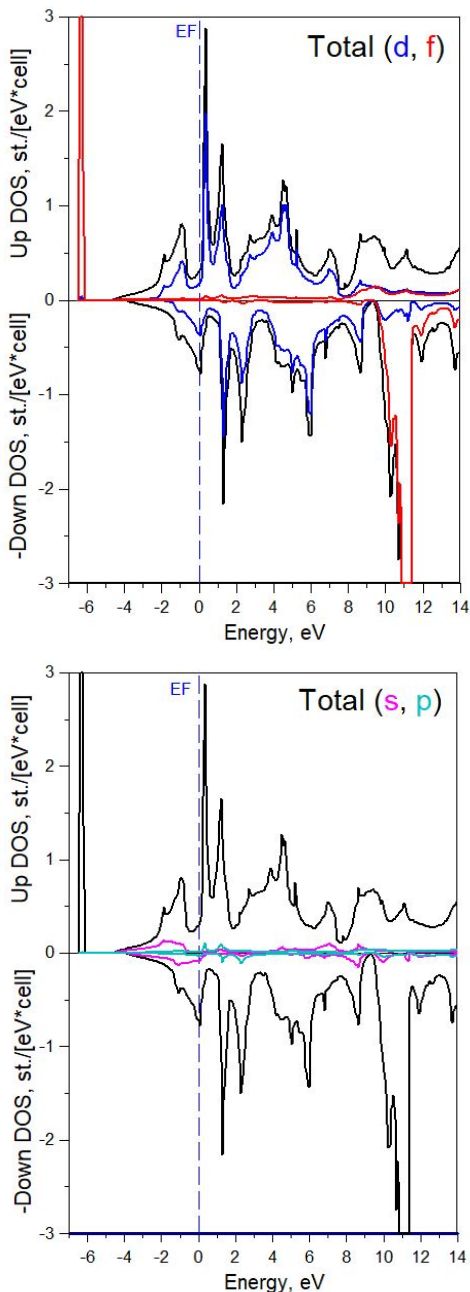


FIG. 2. (Color online) The atomic orbital projected densities of states for (top panel) the Eu d (blue) and f (red) states, and (bottom panel) s (magenta) and p (blue) states, over a broad energy range incorporating both the majority and minority $4f$ bands. Black lines give the total density of states. The spin alignment is ferromagnetic to convey the exchange splitting of the $5d$ bands, and the volume corresponds to zero pressure. The exchange splitting of the d bands around the Fermi level (zero of energy) can be seen to be slightly less than 1 eV.

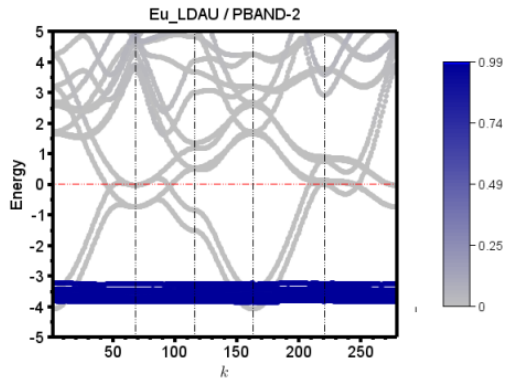


FIG. 3. (color) The band structure of ferromagnetic *bcc* Eu, revealing the exchange splitting of the order of 1 eV of the conduction (Eu $5d$) bands due to Hund's coupling to the Eu $4f$ states. Both spin up and spin down bands are plotted. The colorbar indicates the relative amount of $4f$ (blue) character versus other (gray) character.

$4f^7 J = 7/2 \rightarrow 4f^6 J = 0$ transition, but by some undetermined mechanism.

Because the $4f$ orbitals are highly localized with very small overlap and resulting dispersion (see Fig. 4), magnetic coupling will proceed through the conduction states at the Fermi surface, that is, through generalized RKKY coupling.

E. Spin Waves

Spin waves can be obtained from the exchange interactions and the time evolution of the spin operator given by $\frac{dS_j}{dt} = \frac{i}{\hbar}[H_h, S_j]$, where H_h is the Heisenberg Hamiltonian. For two sublattices in the AFM (*bcc* or *hcp*, but we present results for *bcc*) unit cell the dispersion relation is obtained from the Fourier transformed spin wave expression $S_q = \sum_j S_j e^{i(\vec{q} \cdot \vec{R}_j - \omega t)}$ and the commutation relation among spin operators. The result is simply the diagonalization of a 2×2 matrix (up and down sublattices)

$$\begin{bmatrix} -A_{11}^a(q) + A_{11}^a(0) + A_{12}^b(0) & -A_{12}^a(q) \\ -A_{12}^a(q) & -A_{11}^a(q) + A_{11}^a(0) + A_{12}^b(0) \end{bmatrix},$$

where γ is the sublattice index, $A_{\tau\tau'}^\gamma(q) = S_\gamma J_{\tau\tau'}(q)$ and S_γ is the strength of the moment at sublattice γ . In the AFM case $S_1 = -S_2 \equiv m$, so the spin wave spectrum is

$$\omega(q) = m \sqrt{[J_{11}(q) - J_0]^2 - J_{12}^2(q)}, \quad (1)$$

where $J_0 \equiv J_{11}(0) - J_{21}(0)$. Results for AFM Eu are presented Fig. 5.

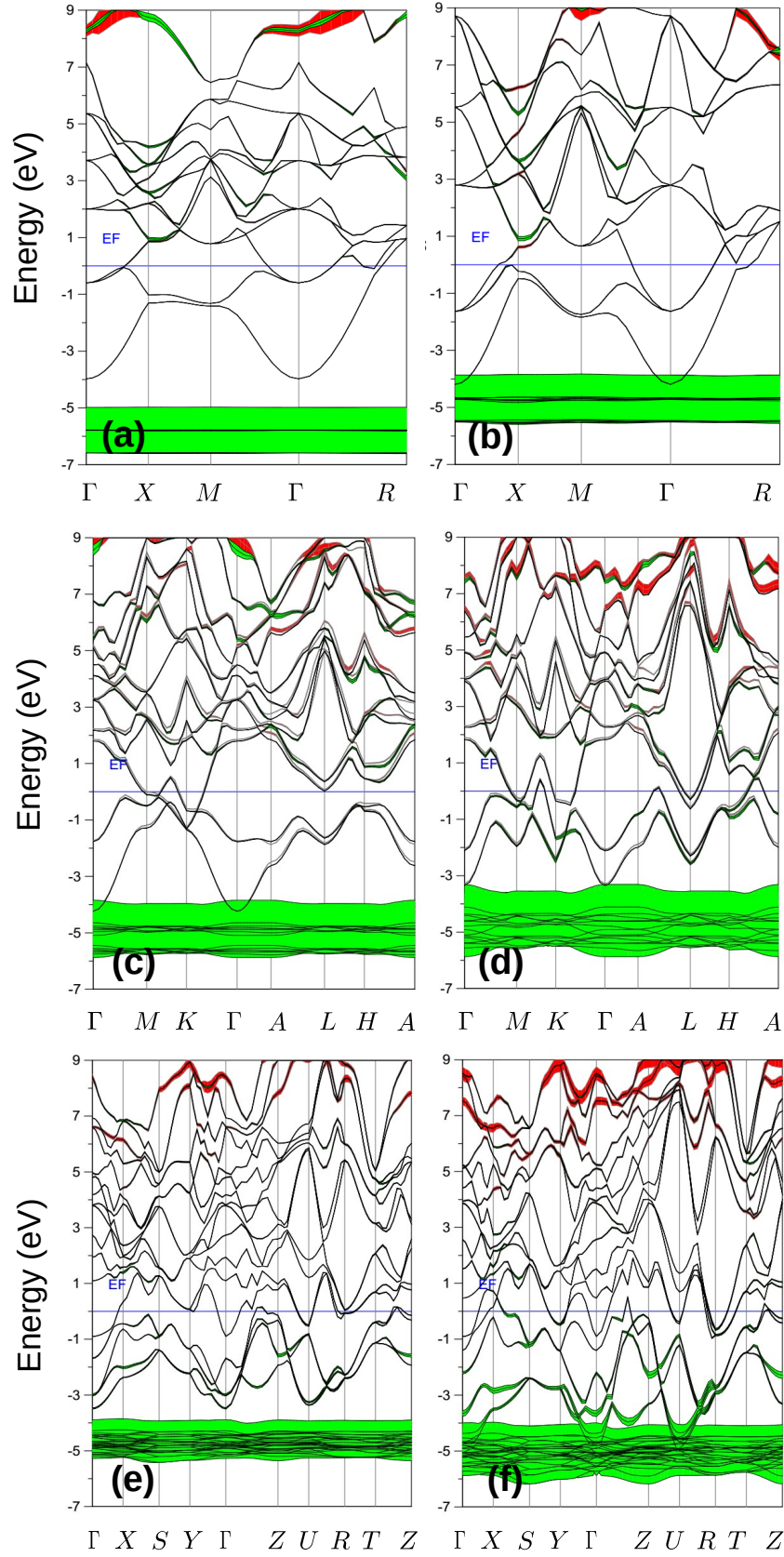


FIG. 4. (Color online) The band structures of AFM Eu metal at different pressure with $U=7$ eV. (a) *bcc* at 0 GPa, (b) *bcc* at 10 GPa, (c) *hcp* at 12 GPa, (d) *hcp* at 37 GPa, (e) *Pnma* at 40 GPa, (f) *Pnma* at 92 GPa. Fat bands (green: spin-up, red: spin-down) are projections on a spin-up site in the AFM order. The occupied $4f$ bands are well below the Fermi level and are fully occupied.

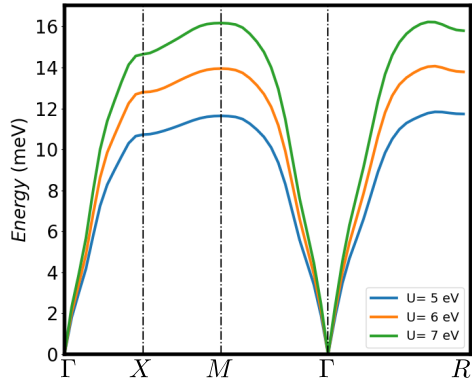
F. $4f - 5d$ Hund's Coupling

FIG. 5. (color) The spin wave spectrum of AFM *bcc* Eu (hence a simple cubic magnetic cell) at ambient pressure along high symmetry lines, with Hubbard U taken as 5, 6, 7 eV respectively. The linear dispersion near Γ is characteristic of AFM order.

The exchange splitting between the Eu $4f$ and $5d$ is obtained from the ferromagnetic band structure shown in Fig. 3. The splitting of the order of 1 eV near the Fermi level provides the magnitude of the intra-atomic $4f - 5d$ exchange splitting quoted in the main text.